ASPECT: The Algebraic Speckle Tomography technique for enhanced phase contrast imaging

Alessandro Mirone,[1*] Ludovic Broche,[1] Emmanuel Brun[2]

[1]ESRF, the European Synchrotron, Grenoble, 38000, France.; [2]Inserm UA7 Strobe, Université Grenoble Alpes, Grenoble, 38000, France.
*Corresponding author: mirone@esrf.fr

ABSTRACT
We present Aspect: a new reconstruction technique for x-ray phase-contrast tomography which faithfully implements the physics of geometric optics in the forward model. The code works in both weak and strong phase effects regimes. The beam is decomposed into an array of sub-pixel gaussian beamlets which are deflected and attenuated according to the sample optical index. The voxels phase contributions and absorptions are found by fitting at once the detector pixels intensities at all rotation angles. We show experimental results obtained at synchrotron and conventional sources with speckles, and perform modelling of a clinical application considering speckle and edge-illumination setups.

Keywords: Phase Retrieval; Speckle Based Imaging; Edge illumination; X-ray Phase Contrast Imaging; Low Dose.

1. INTRODUCTION

In x-ray phase contrast imaging, the phase contrast, enhanced by the experimental setup, complements the X-ray absorption contrast and allows a better visibility of the different tissues. Its possible clinical application for reducing the absorbed dose, at equivalent signal/noise ratio, is the subject of intense research[1].

To enhance the phase contrast, propagation techniques exploit the interference between different parts of the beam after interaction with the sample. On conventional sources, where coherence lengths are short, the interference fringes are smeared out[2]. However the geometric-optic effect of phase transverse derivatives remains, in particular the focussing-defocussing effect of the second derivatives (lensing effect) and the shift effect of the first derivatives (prism effect)[3]. The x-ray δ/β ratios being positive, the lens term acts at increasing the brightness(darkness) of a transparent(absorbing) feature by focussing(defocussing). This effect first increases with the detector-to-sample distance, then saturates for distances greater than the source-to-detector distance, due to magnification and blurring (finite source size) of the imaged features[4]. Practical reasons prevent anyway larger distances. To enhance further the phase signal the prism effect can be highlighted by inducing strong transverse beam intensity modulations and observing their shifts after interaction with the sample. In this regard we contemplate two recent lines of research. One is the edge illumination technique, with subpixel beamlets whose shifts are read through the illumination variation of sub-pixel masked areas of the detector[5] . The second technique is speckle imaging[6], where the modulations are relatively large, covering one or few pixels in extent. Our tool is a new revolutionary reconstruction method with a unifying formalism which:

- is based on a forward model which is exact within geometrical optics and valid at all regimes of either weak or strong phase effects (several pixels shifts)
- obtains self-consistently phase, absorption and (optionally) the ultra-small-angle scattering directly in the volume representation. The retrieval is robust thank to the phase gradient localisation on the features borders (2D structures) at variance of being diluted over all projections as in the projection representation.

We have :

- (on synchrotron) got strong improvements of the reconstructed images and gone beyond the limits of current methods which assume small shifts.
- (on conventional sources) applied successfully our method using speckles in cone geometry.
- reconstructed a numerical knee mockup, optimising speckle and edge illumination setups and imaged small fractures in the joint cartilage at low dose.

2. STATE OF THE ART

Speckles and edge illumination techniques can be considered as two different optimisations of the same problem. The speckle setup is easily performed with a random mask that does not need any particular alignment. The beam modulation for edge-illumination is obtained instead by a regular grid of transparent windows opened in an absorbing mask. Each window selects a beamlet which illuminates, in the absence of the sample induced shifts, the border (edge) between an active area of a pixel and a masked region. The masked regions are obtained by a second grid mask. This setup imposes strict conditions on the alignment but optimises the "usefulness" of the filtered photons: being close to an edge their signal is less "predictable" when small shifts (shifts are small in clinical setups) make them being detected or masked. The removed photons are instead those which would have impinged, far from the edge, the pixel active area regardless of the shift, thus bringing no information but only quantum noise in the limit where phase effects prevail on absorption ones. For both techniques the phase retrieval is performed projection by projection. For speckle tomography the inversion of a two dimensional Poisson equation, after discarding some non translation invariant factors[8], replaces the piece-wise correlation method[6] to circumvent its coarsening effect. For edge illumination, instead, the retrieval is done pixel by pixel and requires several measures at different detector translations, to detect the shift (assumed locally constant), the height of the beamlet and (optionally) the ultra-small-scattering[9].
Beside the different details and approximations of the retrieval procedures we retain that the information redundancy existing between projections and between pixels still remains to be exploited. This is the focus of our method.

3. BREAKTHROUGH CHARACTER OF THE PROJECT

Both experimental setup and reconstruction method can be optimised when correlation between different parts of the dataset exists. As an example, fig 1a sketches a standard edge-illumination setup. The signal of a pixel is to a large extent predictable from the signal of the neighbouring one, the beamlets having travelled nearby, probing similar phase gradients and absorptions in the sample.
In the alternative setup of figure 1b the phase gradient intervenes with an opposite sign on pixel 2 than on pixel 1 and brings new information which helps to disentangle the phase gradient from the absorption.
We fit the whole dataset at all rotation angles at once to get the volume variables which describe the beam-sample interaction. These are the phase contribution $\phi(r)$, the absorption $\mu(r)$ and, optionally, the

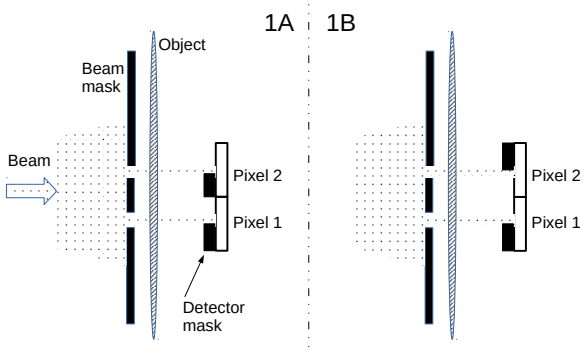

Fig. 1. Two setups with a different information content. In 1A, given an object with low entropy, the pixel 2 signal is, to a large extent, predictible from the pixel 1 signal. In 1B the phase gradient acts with an opposite sign on pixel 2 and its signal is less predictible.

---

ultra-small scattering $\Delta(r)$. The measured non-interacting beam is first re-synthetised expressing its intensity $I_0(x,y)$ on the detector, as an array of beamlets on a uniform subgrid of step d:

$$I_0(x,y)=\sum_{i,j} f_{ij}\exp\left(-\frac{(id-x)^2+(jd-y)^2}{2\sigma^2}\right)$$

with the following relation for the spacing d and width σ :
$d \ll pixel\ size$ and $\sigma > d$.
The f_{ij} are fixed, for the speckles case, interpolating between pixels of the reference image, while for edge illuminations they can be obtained through several detector translation steps and acquisitions. The intensity I_s in the presence of the sample, for rotation angle θ , is obtained substituting σ, i, j, f in I_0 with their primed counterparts

$$I_s(x,y)=\sum_{i,j} f'_{ij}\exp\left(-\frac{(i'd-x)^2+(j'd-y)^2}{2\sigma'^2}\right)$$

with

$$\sigma' = P_S(\theta,\Delta,i,j)$$
$$i' = P_I(\theta,\phi,i,j)$$
$$j' = P_J(\theta,\phi,i,j)$$
$$f'_{ij} = P_F(\theta,\mu,i,j)f_{ij}$$

where P_S accounts for the widening due to ultra-small scattering (if neglected $P_S=\sigma$), the prism terms are accounted for by P_I, P_J and the absorption by P_F . The lensing term is implicit: I_s is proportional to the local density, at a detector position, of the impact points (i', j') . The variables Δ, ϕ, μ are given on the volume voxels, whose step approximatively matches by projection the detector pixels size. The P functions are first calculated

for the pixel centres, and then interpolated for the subgrid points (i,j). Given the function $I_s(x,y)$ the measured intensity $I_M(ix,iy)$ at pixel (ix,iy) is given by the acceptance operator $A_{ix,iy}$ which gives the intensity integral over the pixel active area:

$$A_{ix,iy}(I_s)=\int a_{ix,iy}(x,y)I_s(x,y)\,dx\,dy$$

where $a_{ix,iy}(x,y)$ is zero outside the acceptance region. The operator is implemented, assuming sharp borders, as sum of products of erf functions. We solve

$$\underset{\Delta,\phi,\mu}{argmin}\{C(\Delta,\phi,\mu)+\sum_{ix,iy,\theta}\frac{(A_{ix,iy}(I_s)-I_M(ix,iy))^2}{I_M(ix,iy)}$$

where C stands for the regularisation and constraint terms which are:

$$C(\Delta,\phi,\mu)=\beta_\phi TV(\phi)+I_0(\phi-R\mu)$$

where TV is the total variation and I_0 is the indicator function of the $\{0\}$ set which enforces the linear relationship $\phi=R\mu$. For an homogenous sample R is a scalar, while for a segmented sample it can be a diagonal matrix wich is constant over homogenous sub-regions.

4. PROJECT RESULTS

Our method does not depend on any specialised simplification and is therefore an ideal tool to perform comparative reconstructions and optimisations on all experimental setups which can be described by geometric optics. We present applications to conventional sources, with speckles as well as on edge-illumination setups, and to synchrotron sources.

4.1. Synchrotron test

We show in fig 2 the reconstruction of a mouse knee from synchrotron data from ESRF ID17 beamline[10] using a pink beam ($\Delta E/E\simeq 20\,KeV/40\,KeV$), and a standard (no speckles) strong propagation enhancement of phase effects. The prism shifts, in the Aspect calculation, ranged up to beyond 4 pixels for those x-ray travelling tangentially to the surfaces of the bone structures, where the gradients are strongest. It is a setup adapted to enhance, by a strong propagation effect, the phase contrast of the different tissues: ligaments, cartilage, fat and muscles which are shown in Fig. 2 with an adjusted colormap to see the soft tissues. The bones regions remain saturated in white. In Fig. 2a we show the Aspect reconstruction while Fig. 2b is obtained applying first the Paganin phase retrieval[11] and then filtered back-projection. This procedure is routinely applied for this kind of setups and relies on the linearisation of transfer of intensity equations, which is valid for small shifts. Streak artefacts are visible in Fig. 2b and seem to irradiate from the bones. In the Aspect reconstruction these artefacts have almost completely disappeared. We interpret these artefacts as a result of the large shifts which originate from the bone structure. These shifts are correctly accounted for in Aspect, and their removal is an encouraging signal that phase contrast can be further pushed to unprecedented levels on synchrotrons thank to their correct treatment.

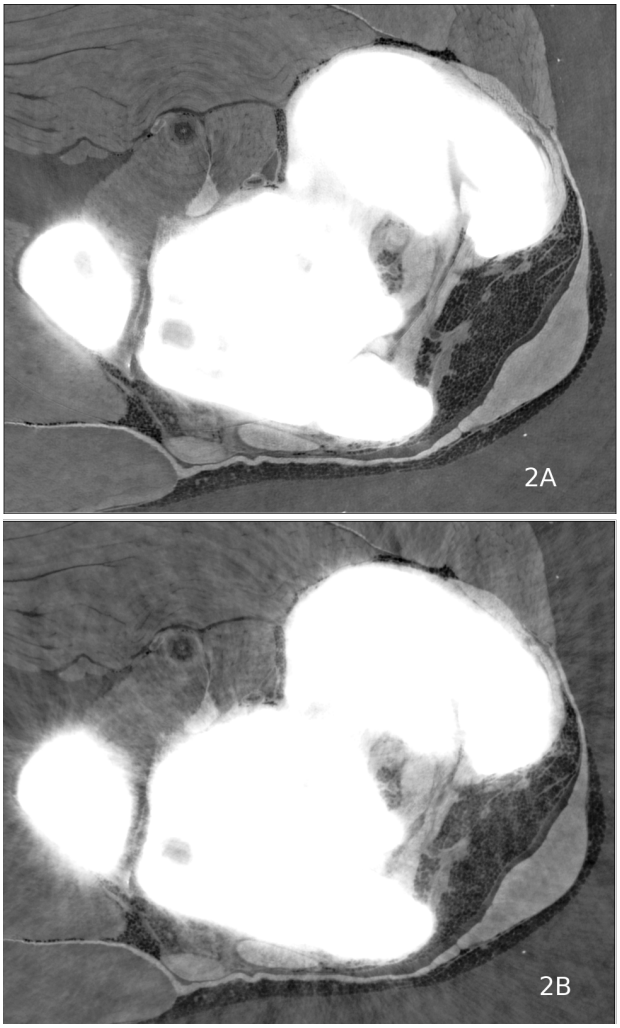

Fig. 2. The Aspect code (2A), faithfully implementing the geometric optic equations, properly inverts the beam-sample interaction even for shifts so large (several pixels) that standard procedures (2B) based on the linearisation of transfer equations are broken and produce streak artefacts.

4.2. Test on a conventional source.

We have performed the speckles tomography of a zebra fish embryo contained in a paraffin block. The

experimental setup consisted in a x-ray source, 30um wide with 12KeV average energy, the rotating axis at 10cm from the source, and a photon counting detector at 70cm from the sample with 75um wide pixels. We show in Fig. 3c one radiography where one can distinguish the gross shape of the paraffin block and, on a finer scale, the speckles induced by the mask. In Fig. 3a we show a slice of the reconstruction performed with Aspect where one can distinguish the embryo. As a comparison we show in figure 3b the same tomography, performed with the same dose but without speckles, and reconstructing with a filtered back projection algorithm. The reconstruction done with Aspect deals correctly with the phase effects which are present in this conventional setup. The prism term produces here shifts of the order of a tenth of a pixel, which give a not negligible signal also through the lensing term. The improvement that we obtain with the Aspect code derives from the correct treatment of both prism and lensing phase effects and this validates the application of Aspect to cone-geometry conventional sources.

4.3. Optimisation of a speckle and an edge-illumination setup for knee tomography.

Fig. 4 shows a slice of a numerical mock-up of a knee (4a). The bones (in white) are in the middle of a 7cm diameter cylinder simulating soft tissues (absorption 0.18cm^{-1}) and cartilage (0.2cm^{-1}). The inset is centred over a horizontal fracture in the cartilage. The photon average energy is 60KeV, the source-object distance is 1m while the detector is at 1m from the object and has 125μm wide pixels. By adding quantum noise we have generated different datasets which correspond to different absorbed doses. We have also considered different setups: edge illumination, speckles, and a flat (non modulated) beam. The different combinations of absorbed dose and beam modulation setup are summarised by showing the fracture inset on different lines and columns, for the different doses and modulation setups. In the first column on the left we show the reconstruction done with Aspect for a flat beam setup (no modulation). The remaining three columns on the right correspond to edge illumination for three different slit widths and source sizes. In the edge illumination setup the slits are parallel to the rotation axis and the source is an ellipsoid with the long axis parallel to the rotation axis. The phase contrast enhancement depends on the source image width, perpendicularly to the slit. This width depends on bot the slit width and the source short axis. Considering our 1:1 setup this effective width is: $w_{eff}^2 = 4\,w_{slit}^2 + w_{source}^2$. The three columns are given for $w_{eff} \simeq 24,12,7\,\mu m$. For this clinical setup the prism shift is very low, of the order of one hundredth of pixel, and even simulating an extreme speckle mask the prism signal was not strong

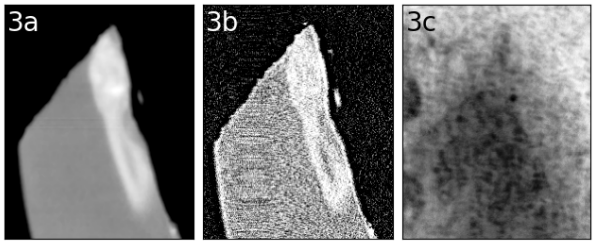

Fig. 3. Reconstruction of a zebra fish embryo in a paraffine block. 3a) Aspect code with speckles data. 3b) Filtered back-projection of non-speckles data. 3c) One radiography with speckles.

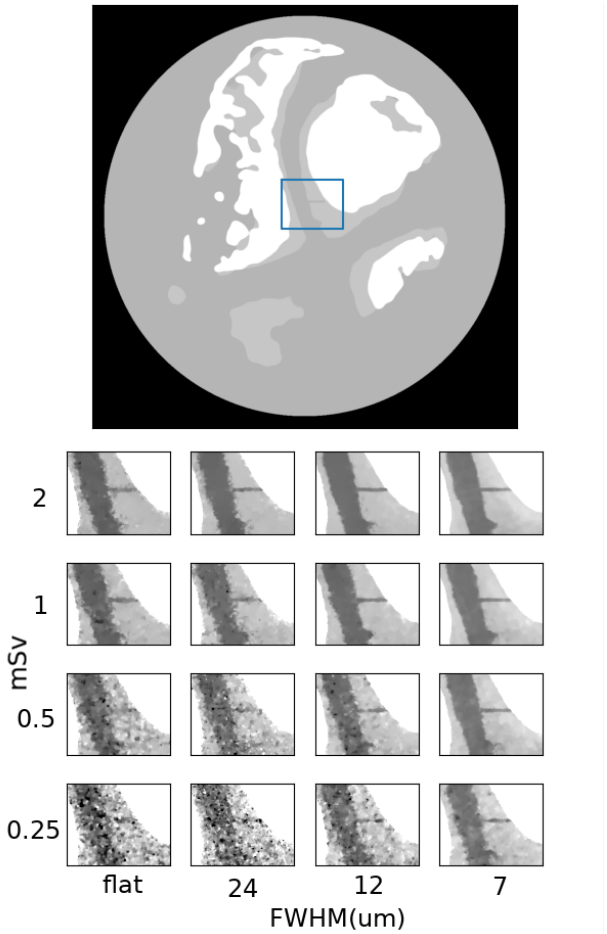

Fig. 4: reconstruction, with Aspect, of a knee joint at different doses, and different FWHM of the beam modulation in edge illumination.

---

enough . With speckles the modulation length cannot go below the pixel size. The improvement is instead dramatic with edge illumination and the cartilage fracture is visible with absorbed dose down to a dose of 0.25mSv. For a real sample, containing more information than our phantom, which has large constant regions, the required dose would be higher, but the dose reduction, obtained with edge illumination, would be the same. Our calculation accounts for both source size and

slit width. The phase enhancement can be increased by decreasing the effective width, as far as it is permitted by the mask technology and detector physics.

5. FUTURE PROJECT VISION

The goals of phase 1 have been fully accomplished and the developed technique, Aspect, allows to extract the maximum information from the data and to faithfully simulate speckle and edge illumination setups. Our tests on a setup for histological samples show pronounced phase effects with shifts of up to tenths of pixel which can be exploited with both speckle and edge illumination setups. On clinical setups, instead, the shifts (in pixel units) are lower by one magnitude order, and only pushing the modulation to the sub-pixel domain, with edge illumination setups, we can drastically reduce the absorbed dose. For the future we will focus, in the short term, on histological setups, while in the medium term we will focus on radiological applications for which the requirements on modulation length and the gantry stability are stricter.

5.1. Technology Scaling

The first step will be the configuration of a tomography apparatus to work on small histological samples using photon energy in the range of 8-30KeV. For this setup the source and the detector are not moving and this is favourable for the mechanical stability. During this first phase we will study the mechanical requirements for the second step with radiological setups based on a rotating gantry and higher energy. The implementation of TRL6-9 will start, for histological setups, as soon as step one is completed. While histological setups can profit of adaptable resolution and darkfield extraction allowed by speckles, the clinical apparatus would be drastically more efficient by considering an edge illumination setup.

5.2. Project Synergies and Outreach

For the development of radiological application with edge illumination we are strongly favorable to join our efforts with Prof. Alessandro Olivo and coworkers for their know-how with masks and detectors and for having initiated the x-ray edge illumination technique. For the histological set-up an industrial partner has been identified for the following TRL 6-9.

6. ACKNOWLEDGEMENT

Authors are grateful to Xenocs for lending the X-ray source and detector and to Sabine Rolland du Roscoat for the access to 3SR platform and her help during the experiment.

This project has received funding from the ATTRACT project funded by the EC under Grant Agreement 777222.

7. REFERENCES

[1] Bravin, A., Coan, P. & Suortti, P. X-ray phase-contrast imaging: from pre-clinical applications towards clinics. Phys. Med. Biol. 58, R1–R35 (2013).
[2] F. Arfelli et al., Low-dose phase contrast X-ray medical imaging,’Phys. Med. Biol. 43, 2845–2852 1998.
[3] Paganin,D.,M.&Pelliccia,D. Tutorials on X-ray Phase Contrast Imaging. arXiv:1902.00364
[4] Paul C. Diemoz, Fabio A. Vittoria, and Alessandro Olivo, "Spatial resolution of edge illumination X-ray phase-contrast imaging," Opt. Express 22, 15514-15529 (2014)
[5] A. Olivo and R. Speller, “A coded-aperture approach allowing x-ray phase contrast imaging with conventional sources,” Appl. Phys. Lett. 91, 074106 (2007).
[6] Berujon, S., Ziegler, E., Cerbino, R. & Peverini, L. Two-Dimensional X-Ray Beam Phase Sensing. Phys. Rev. Lett. 108, 158102 (2012).
[7] Morgan, K. S., Paganin, D. M. & Siu, K. K. W. X-ray phase imaging with a paper analyzer. Appl. Phys. Lett. 100, 124102–124104 (2012).
[8] Paganin,D.,M., Labriet,H.,Brun,E.,Berujon,S. Single-image geometric-flow x-ray speckle tracking Physical Review A 98, 053813 (2018)
[9] Zamir,A., Endrizzi,M., Hagen,C.,K., Vittoria,F.,A., Urbani,L., De Coppi,P.,Olivo,A. Robust phase retrieval for high resolution edge illumination x-ray phase-contrast computed tomography in non-ideal environments Scientific reports 6 (1), 1-9 (2016)
[10] Mittone, A., Fardin, L., Di Lillo, F., Fratini, M., Requardt, H., Mauro, A., Homs-Regojo, R. A., Douissard, P.-A., Barbone, G. E., Stroebel, J., Romano, M., Massimi, L., Begani-Provinciali, G., Palermo, F., Bayat, S., Cedola, A., Coan, P. & Bravin, A. (2020). J. Synchrotron Rad. 27.
[11] Paganin, D., Mayo, S.C., Gureyev, T.E., Miller, P.R. and Wilkins, S.W. (2002), Simultaneous phase and amplitude extraction from a single defocused image of a homogeneous object. Journal of Microscopy, 206: 33-40. (2002)